



Effect of nanoparticle size on magnetic damping parameter in $\text{Co}_{92}\text{Zr}_8$ soft magnetic films

Gaoxue Wang, Chunhui Dong, Changjun Jiang*, Guozhi Chai, Desheng Xue

Key Laboratory for Magnetism and Magnetic Materials of MOE, Lanzhou University, Lanzhou 730000, People's Republic of China

ARTICLE INFO

Article history:

Received 18 December 2011

Received in revised form

23 March 2012

Available online 1 May 2012

Keywords:

Soft magnetic film

Magnetic damping parameter

Nanoparticle size

Sputtering

ABSTRACT

$\text{Co}_{92}\text{Zr}_8(50 \text{ nm})/\text{Ag}(x)$ soft magnetic films have been prepared on Si (111) substrates by oblique sputtering at 45° . Nanoparticle size of $\text{Co}_{92}\text{Zr}_8$ soft magnetic films can be tuned by thickening Ag buffer layer from 9 nm to 96 nm. The static and dynamic magnetic properties show great dependence on Ag buffer layer thickness. The coercivity and effective damping parameter of $\text{Co}_{92}\text{Zr}_8$ films increase with thickening Ag buffer layer. The intrinsic and extrinsic parts of damping were extracted from the effective damping parameter. For $x=96 \text{ nm}$ film, the extrinsic damping parameter is 0.028, which is significantly larger than 0.004 for $x=9 \text{ nm}$ film. The origin of the enhancement of extrinsic damping can be explained by increased inhomogeneity of anisotropy. Therefore, it is an effective method to tailor magnetic damping parameter of thin magnetic films, which is desirable for high frequency application.

© 2012 Elsevier B.V. All rights reserved.

1. Introduction

Soft magnetic films with excellent high frequency characteristics are a promising material for use in magnetic components such as data transmission and multiple access devices [1–5]. The magnetic film for application is usually based on the analysis of their dynamic magnetic properties or the precession of magnetization subjected to an effective magnetic anisotropy field H_{eff} as given by the Landau–Lifshitz–Gilbert (LLG) [6] equation

$$\frac{d}{dt} \mathbf{M} = -\gamma \mathbf{M} \times H_{\text{eff}} + \frac{\alpha_{\text{eff}}}{4\pi M_s} \left(\mathbf{M} \times \frac{d}{dt} \mathbf{M} \right), \quad (1)$$

where γ is the gyromagnetic ratio, $4\pi M_s$ is the saturation magnetization of the film, and \mathbf{M} represents the magnetization vector. The first term in Eq. (1) describes the precession of \mathbf{M} along H_{eff} . The second term in Eq. (1) is phenomenological in nature, which describes the magnetic energy dissipation. According to the LLG equation, the key parameters which determine the dynamic magnetic properties of the soft magnetic films are the magnetic anisotropy field H_{eff} , saturation magnetization $4\pi M_s$ and the effective damping parameter α_{eff} .

The effective damping parameter α_{eff} controls how rapidly the magnetization reaches equilibrium position in the absence of external stimulus. This makes α_{eff} an important parameter in the description of dynamic property in magnetic materials. Several techniques were employed to realize the adjustable damping parameter, among the techniques were doping transition metals

[7,8], depositing multilayers [9], and diluting the ferromagnetic (FM) material [10]. The contribution to effective damping parameter often falls into two parts: intrinsic and extrinsic. The intrinsic part comes from the Gilbert-like damping, the extrinsic part has its origin in anisotropy dispersion [11] and magnon scattering [12].

The effect of nanoparticle size on the magnetic properties of magnetic films such as coercivity and magnetoresistance has always been an intriguing subject in the field of thin film magnetism. From a technological point of view, nanoparticle size effects are of importance because they significantly influence the way in which thin films can be applied for magnetic recording and magneto-electronics. However, previous studies have mainly focused on nanoparticle size induced changes of static magnetic properties of ferromagnetic films [13,14], effect of nanoparticle size on magnetization dynamics has been seldom discussed.

In this paper, we investigate effect of nanoparticle size on magnetic damping parameter in $\text{Co}_{92}\text{Zr}_8$ soft magnetic films. We show that the nanoparticle size of $\text{Co}_{92}\text{Zr}_8$ film can be systematically tuned by changing Ag buffer layer thickness. An enhancement of α_{eff} is achieved by thickening Ag buffer layer from 9 nm to 96 nm, the origin of the enhancement is increased inhomogeneity of anisotropy, which results in significantly larger extrinsic damping parameter α_{ext} of 0.028 for $x=96 \text{ nm}$ film than 0.004 for $x=9 \text{ nm}$ film.

2. Experimental procedure

The $\text{Co}_{92}\text{Zr}_8(50 \text{ nm})/\text{Ag}(x)$ ($x=9, 22, 35, 53, 78, 83$, and 96 nm) films were deposited on Si(111) substrates at room temperature

* Corresponding author.

E-mail address: jiangchj@lzu.edu.cn (C. Jiang).

by radio frequency sputtering, with background pressure lower than 5×10^{-5} Pa. An Ag target, 70 mm in diameter and 3 mm in thickness, was used to deposit Ag buffer layer; and a Co target, the same size as Ag target, on which Zr chips were placed in a regular manner, was used to deposit $\text{Co}_{92}\text{Zr}_8$ soft magnetic layers. All the films were deposited at an angle of 45° to attain in-plane uniaxial anisotropy. The working Ar pressure was 0.3 Pa with an Ar flow rate of 80 SCCM (SCCM denotes cubic centimeter per minute at STP), the radio frequency power density was 2.5 W/sc. The compositions were measured by energy dispersive x-ray spectroscopy (EDS). The static magnetic properties were determined by vibrating sample magnetometer (VSM). The permeability were carried out with a PNA E8386B network analyzer based on microstrip method and in-plane ferromagnetic resonance (FMR) measurements were performed in a JEOL, JES-FA 300 (X-band at 8.969 GHz) spectrometer.

3. Results and discussion

Fig. 1 shows the variation of the nanoparticle size as a function of Ag buffer layer thickness. Inset of Fig. 1 are the high-resolution scanning electron microscopy (SEM) images of single layer Ag films of (a) 9 nm and (b) 75 nm, and (c), (d) SEM images of as-deposited $\text{Co}_{92}\text{Zr}_8(50\text{ nm})/\text{Ag}(x)$ films for $x=9$ and 75 nm. It can be clearly seen that nanoparticle size of $\text{Co}_{92}\text{Zr}_8$ films depends on the morphology of Ag buffer layer. Thickening Ag buffer layer induces larger nanoparticle size in $\text{Co}_{92}\text{Zr}_8$ films. Thus, nanoparticle size of $\text{Co}_{92}\text{Zr}_8$ films can be tuned by thickening Ag buffer layer from 9 nm to 96 nm. Nanoparticle size increases gradually for x less than 75 nm films, and experiences a rapid increase for $x=83$ and 96 nm films.

Fig. 2 shows the in-plane hysteresis loops of the as-deposited $x=9$ nm and 96 nm films measured at room temperature. The coercivity of $x=96$ nm film is much larger than that of $x=9$ nm film, difference in the hysteresis loops measured along the easy axis (EA) and the hard axis (HA) exhibits an in-plane uniaxial magnetic anisotropy. The Ag buffer layer thickness dependence of coercivity is summarized in Fig. 3. The coercivity tends to increase as thickness of Ag buffer layer increases. The increase of coercivity can be illustrated by the increased nanoparticle size induced by thickening Ag buffer layer. Ag tends to segregate at the grain boundary of $\text{Co}_{92}\text{Zr}_8$, and increases the grain boundary energy, which results in the enhancement of the coercivity [15].

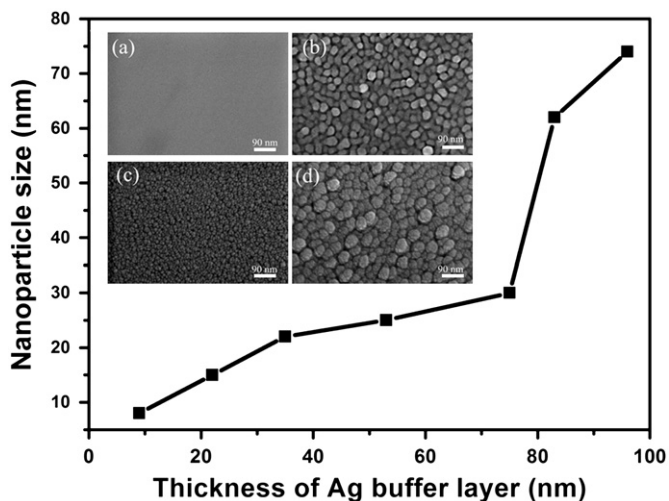


Fig. 1. The variation of nanoparticle size as a function of Ag buffer layer thickness. Insets are SEM images of single Ag film of (a) 9 nm, (b) 75 nm, and (c), (d) SEM images of as-deposited $\text{Co}_{92}\text{Zr}_8(50\text{ nm})/\text{Ag}(x)$ films for $x=9$ nm $x=75$ nm.

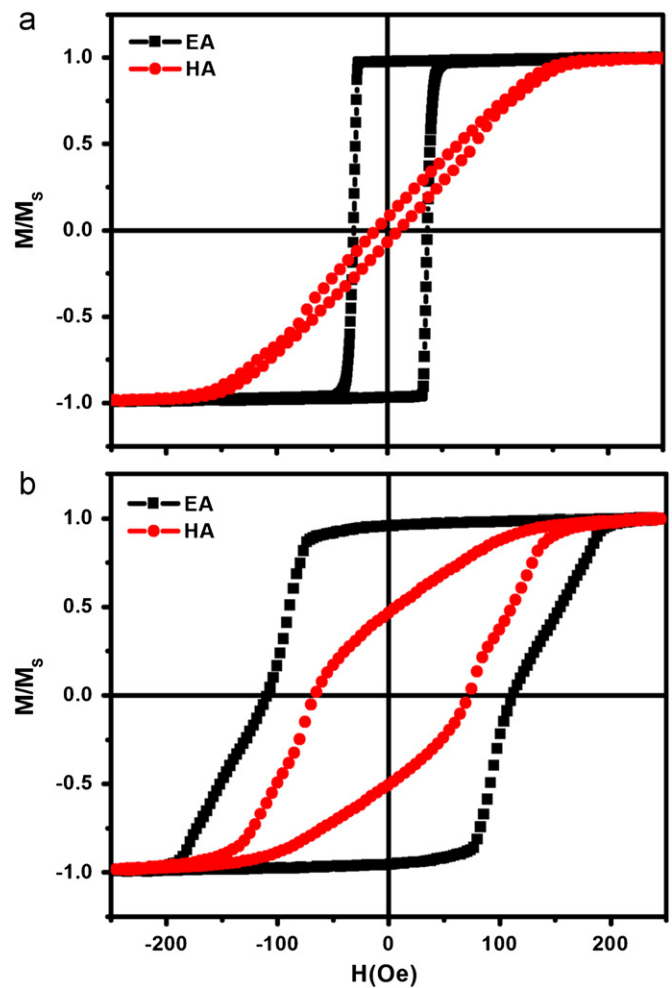


Fig. 2. In-plane hysteresis loops of (a) $x=9$ nm film and (b) $x=96$ nm film. (EA is parallel to easy axis of uniaxial anisotropy, and HA is hard axis).

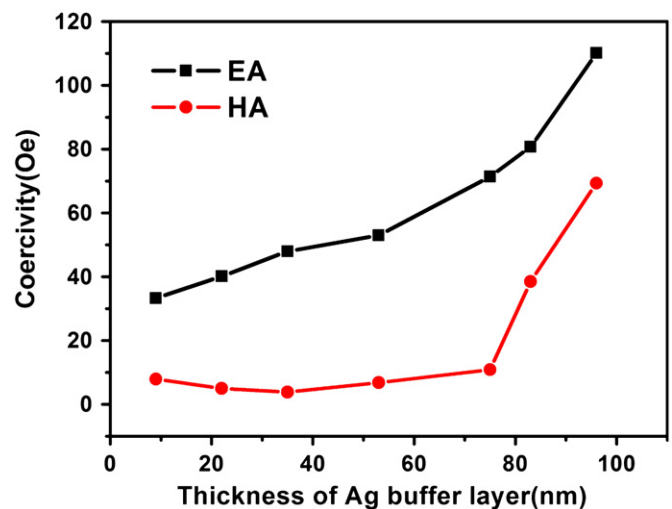


Fig. 3. Coercivity H_c of $\text{Co}_{92}\text{Zr}_8(50\text{ nm})/\text{Ag}(x)$ films as functions of Ag buffer layer thickness.

In order to obtain saturation magnetization $4\pi M_s$ and effective magnetic anisotropy field H_{eff} , we measured the angle dependence of in-plane FMR, all the spectra were taken at 8.969 GHz. The resonance field dependence of the resonance frequency for homogenous precession in the limit of $H_r + H_{eff} \ll M_s$ is expressed

by the Kittel formula [16] as

$$f_r^2 = \frac{\gamma}{2\pi} f_M \mu_0 (H_r + H_{eff} \cos(2\theta)), \quad (2)$$

where $f_M = \gamma M_S / 2\pi \mu_0$, μ_0 is the vacuum permeability, H_r is the resonance field. According to Eq. (2), H_r can be expressed as a function of $\cos(2\theta)$. By fitting the angle dependence of resonance field curve, $4\pi M_S$ and H_{eff} can be obtained. Fig. 4 is an example of the fitting procedure for $x=96$ nm film. Square dots represent experimental results, and solid line is the fitting curve by Eq. (2). Resonance field H_r of FMR is defined as the intersection of Lorentz line with the abscissa, as shown in the inset of Fig. 4. If we took $\gamma / 2\pi \mu_0 = 28$ GHz/T, the saturation magnetization $M_S = 1.45$ and 1.38 T, then, the effective magnetic anisotropy field $H_{eff} = 142$ and 128 Oe for $x=9$ and 96 nm films can be obtained, respectively. The values of static M_S obtained by VSM measurement for $x=9$ and 96 nm films are 1.48 and 1.43 T, respectively, which are in close agreement with the dynamic M_S obtained by FMR. The slight difference can be explained by surface anisotropy [17,18].

Fig. 5 shows permeability spectra of $x=9$ and 96 nm films measured by the microstrip method using PNA E8363B vector network analyzer [19], where μ' and μ'' represent the real and imaginary part of complex permeability, respectively. The permeability spectra have obvious dependence on Ag buffer layer thickness, indicated by shifting of resonance frequency and broadening of full width at half maximum (FWHM) of the imaginary complex permeability. Based on LLG equation, the permeability of thin film can be described as [20]

$$\mu = 1 + \frac{f_m(f_0 + f_m + i\alpha_{eff}f)}{f_r^2 - f^2 + if\Delta f_r}, \quad (3)$$

where $f_m = \gamma 4\pi M_S / 2\pi$, $f_0 = \gamma H_{eff} / 2\pi$, $f_r^2 = f_0^2 + f_m f_0$, and $\Delta f_r = \alpha(2f_0 + f_m)$. Taken $4\pi M_S$ and H_{eff} values from fitting results of Eq. (2), all the experimental permeability spectra can be fitted with Eq. (3). The fitted results of effective damping parameter α_{eff} were shown in Fig. 6. The effective damping parameter α_{eff} for $x=96$ nm film is about 0.037, which is larger than 0.010 for $x=9$ nm film.

The contribution to effective damping parameter often falls into two parts: intrinsic and extrinsic. The intrinsic part comes from the Gilbert-like damping, the extrinsic part has its origin in anisotropy dispersion and magnon scattering. In order to understand the origin of the enhancement of effective damping

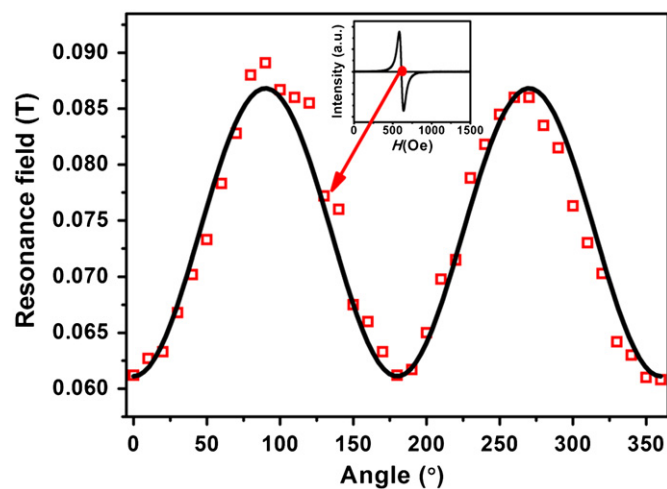


Fig. 4. Resonance fields as functions of angle between external magnetic field and in-plane easy axis of $x=96$ nm film (square dots represent experimental results, and solid line is fitting curve by Eq. (2)). The inset shows the in-plane FMR curve at the angle of 130° .

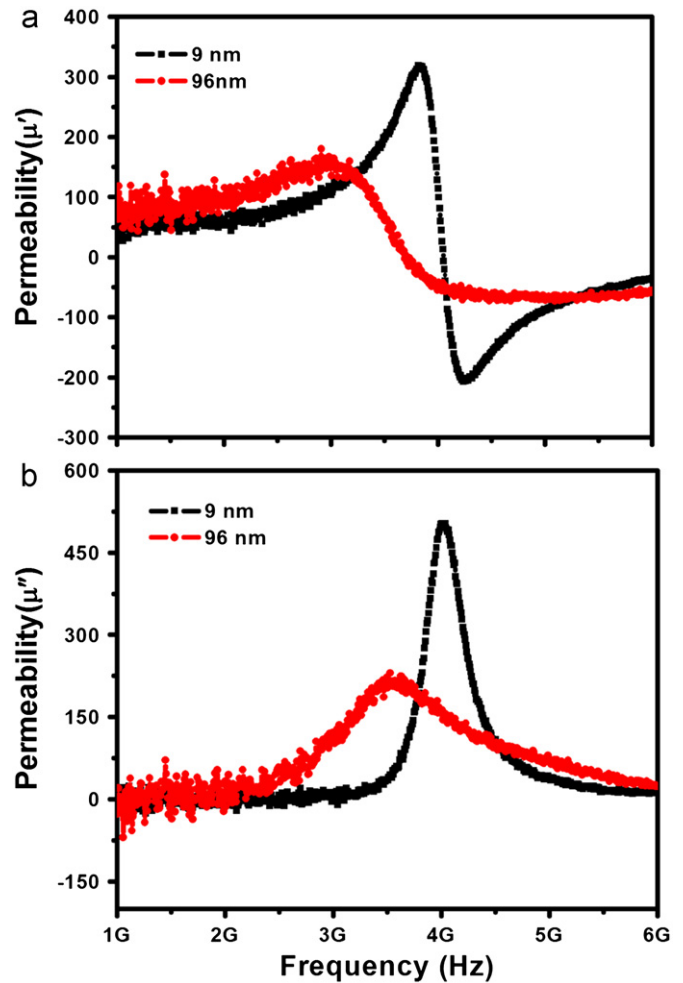


Fig. 5. Frequency dependence of (a) the real μ' and (b) the imaginary μ'' parts of permeability for $x=9$ and 96 nm films, respectively.

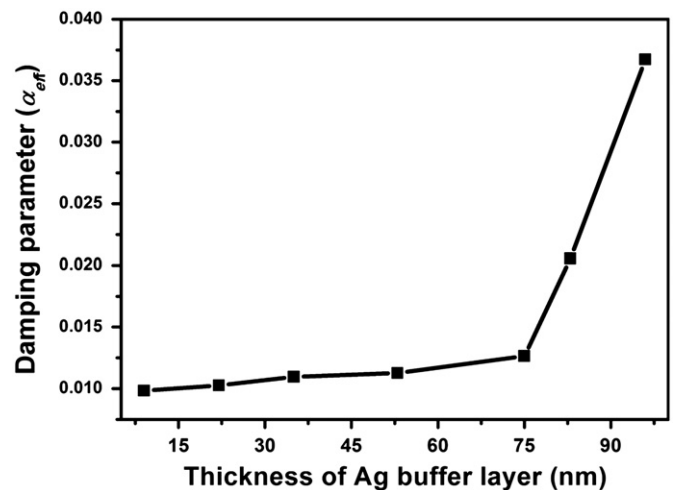


Fig. 6. Anisotropy fields and the effective damping parameters of $\text{Co}_{92}\text{Zr}_8$ (50 nm)/Ag (x) films vs. Ag buffer layer thickness.

parameter in our cases, a method proposed by de Sihues et al. [21] was used to extract the intrinsic part of effective damping parameter. The linewidth of FMR of thin magnetic films can be

Table 1The fitted results of α_{eff} , α_{in} and $\Delta\varphi$ for $x=9$ and 96 nm films, respectively.

	α_{eff}	α_{in}	α_{ext}	$\Delta\varphi$ (deg.)
Co ₉₂ Zr ₈ (50 nm)/Ag(9 nm)	0.010	0.006	0.004	0.007
Co ₉₂ Zr ₈ (50 nm)/Ag(96 nm)	0.037	0.009	0.028	0.031

expressed as

$$\Delta H \cong \frac{2}{\sqrt{3}} \frac{G}{\gamma^2 M} \frac{\omega}{|\cos(\varphi_0 - \varphi_H)|} + 2H_u \frac{\sin 2(\varphi_0 - \varphi_u)}{\cos(\varphi_0 - \varphi_H)} \Delta\varphi_u + \Delta H(0), \quad (4)$$

where $\Delta\varphi_u$ is the angular dispersion of the uniaxial axis, which can be used to describe the inhomogeneity of in-plane magnetic anisotropy field. Taken the effective anisotropy field and saturation magnetization values, the intrinsic damping parameter and $\Delta\varphi_u$ can be obtained by fitting with Eq. (4). The fitted results for $x=9$ and 96 nm films were shown in Table 1, where α_{eff} is the effective damping parameter; α_{in} is the intrinsic damping parameter; α_{ext} is the subtraction of α_{eff} and α_{in} . For $x=9$ nm film, the effective damping parameter α_{eff} is 0.010, the main contribution to the effective damping parameter comes from intrinsic damping, which is 0.006. For $x=96$ nm film, the extrinsic damping parameter is 0.028, which is larger than 0.004 for $x=9$ nm film. The enhancement of extrinsic damping parameter can be explained by increased nanoparticle size induced inhomogeneity of anisotropy, as indicated by enhancement of $\Delta\varphi_u$ from 0.007 to 0.031 by thickening Ag buffer layer from 9 nm to 96 nm.

4. Conclusions

We have shown that the nanoparticle size has a strong impact on the magnetic damping parameter in soft magnetic films. The nanoparticle size of Co₉₂Zr₈ films can be tuned by changing Ag buffer layer thickness. The coercivity and effective damping parameter monotonically increase as the nanoparticle size increases. The increase of coercivity is due to enhancement of the grain boundary energy. The enhancement of effective damping parameter results from increased inhomogeneity of anisotropy, which leads to significant enhancement of extrinsic damping parameter. It is an

effective way to tailor magnetic damping parameter of thin magnetic films for various applications.

Acknowledgments

This work is supported by the National Basic Research Program of China (Grant no. 2012CB933101), the National Science Fund for Distinguished Young Scholars (Grant no. 50925103), the Keygrant Project of Chinese Ministry of Education (Grant no. 309027), the National Natural Science Foundation of China (Grant nos. 11034004, 50902064 and 51107055), and the Fundamental Research Funds for the Central Universities (Izujbky-2010-74).

References

- [1] Y.W. Zhao, X.K. Zhang, J.Q. Xiao, *Advanced Materials* (Weinheim, Germany) 17 (2005) 915.
- [2] K. Seemann, H. Leiste, V. Bekker, *Journal of Magnetism and Magnetic Materials* 283 (2004) 310.
- [3] Y. Hayakawa, A. Makino, H. Fujimori, A. Inoue, *Journal of Applied Physics* 81 (1997) 3747.
- [4] A. Encinas-Oropesa, M. Demand, L. Piraux, U. Ebels, I. Huynen, *Journal of Applied Physics* 89 (2001) 6704.
- [5] N.N. Phuoc, F. Xu, C.K. Ong, *Applied Physics Letters* 94 (2009) 092505.
- [6] T.L. Gilbert, *IEEE Transactions on Magnetics* 40 (2004) 3443.
- [7] C.J. Jiang, D.S. Xue, D.W. Guo, X.L. Fan, *Journal of Applied Physics* 106 (2009) 103910.
- [8] Z.M. Zhang, M. Lin, J.Y. Zhu, D.W. Guo, G.Z. Chai, X.L. Fan, Y.C. Yang, D.S. Xue, *Journal of Applied Physics* 107 (2010) 083912.
- [9] J. McCord, R. Kaltofen, O.G. Schmidt, L. Schultz, *Applied Physics Letters* 92 (2008) 162506.
- [10] Y. Guan, W.E. Bailey, *Journal of Applied Physics* 101 (2007) 09D104.
- [11] J.O. Rantschler, C. Alexander, *Journal of Applied Physics* 93 (2003) 6665.
- [12] R. Arias, D.L. Mills, *Journal of Applied Physics* 60 (1999) 7395.
- [13] M. Li, G. Wang, H. Min, *Journal of Applied Physics* 83 (1998) 5313.
- [14] C. Yu, W. Cheng, W. Lee, S. Chen, Y. Liou, Y. Yao, *Journal of Applied Physics* 93 (2003) 7468.
- [15] S.C. Chen, P.C. Kuo, C.Y. Chou, A.C. Sun, *Journal of Applied Physics* 97 (2005) 10N107.
- [16] R. Lopusnik, J.P. Nibarger, T.J. Silva, Z. Celinski, *Applied Physics Letters* 83 (2003) 96.
- [17] R. Naik, C. Kota, J.S. Payson, G.L. Dunifer, *Physical Review B* 48 (1993) 1008.
- [18] J.P. Nibarger, R. Lopusnik, Z. Celinski, T.J. Silva, *Applied Physics Letters* 83 (2003) 93.
- [19] N.X. Sun, S.X. Wang, T.J. Silva, *IEEE Transactions on Magnetics* 38 (2002) 146.
- [20] Y. Liu, L.F. Chen, C.Y. Tan, H.J. Liu, C.K. Ong, *Review of Scientific Instruments* 76 (2005) 063911.
- [21] M.D. de Sihues, C. Durante-Rincon, J.R. Fermin, *Journal of Magnetism and Magnetic Materials* 316 (2007) e462.